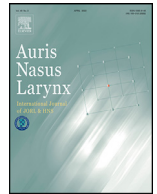




Contents lists available at ScienceDirect

Auris Nasus Larynx

journal homepage: [www.elsevier.com/locate/anl](http://www.elsevier.com/locate/anl)

# Artificial intelligence-based diagnosis of the depth of laryngopharyngeal cancer

Kohei Yumii<sup>a</sup>, Tsutomu Ueda<sup>a,\*</sup>, Daisuke Kawahara<sup>b</sup>, Nobuyuki Chikui<sup>a</sup>, Takayuki Taruya<sup>a</sup>, Takao Hamamoto<sup>a</sup>, Sachio Takeno<sup>a</sup>

<sup>a</sup>Department of Otorhinolaryngology, Head and Neck Surgery, Graduate School of Biomedical and Health Sciences, Hiroshima University, 1-2-3 Kasumi Minami-ku, Hiroshima, Japan

<sup>b</sup>Department of Radiation Oncology, Graduate School of Biomedical Health Sciences, Hiroshima University, Hiroshima, Japan

## ARTICLE INFO

### Article history:

Received 5 July 2023

Accepted 8 September 2023

Available online xxx

### Keywords:

Artificial intelligence (AI)

Head and neck cancer

Transoral surgery

Diagnosis of depth

Radiomics

Deep learning

## ABSTRACT

**Objective:** Transoral surgery (TOS) is a widely used treatment for laryngopharyngeal cancer. There are some difficult cases of setting the extent of resection in TOS, particularly in setting the vertical margins. However, positive vertical margins require additional treatment. Further, excessive resection should be avoided as it increases the risk of bleeding as a postoperative complication and may lead to decreased quality of life, such as dysphagia. Considering these issues, determining the extent of resection in TOS is an important consideration. In this study, we investigated the possibility of accurately diagnosing the depth of laryngopharyngeal cancer using radiomics, an image analysis method based on artificial intelligence (AI).

**Methods:** We included esophagogastroduodenoscopic images of 95 lesions that were pathologically diagnosed as squamous cell carcinoma (SCC) and treated with transoral surgery at our institution between August 2009 and April 2020. Of the 95 lesions, 54 were SCC *in situ*, and 41 were SCC. Radiomics analysis was performed on 95 upper gastrointestinal endoscopic NBI images of these lesions to evaluate their diagnostic performance for the presence of subepithelial invasion. The lesions in the endoscopic images were manually delineated, and the accuracy, sensitivity, specificity, and area under the curve (AUC) were evaluated from the features obtained using least absolute shrinkage and selection operator analysis. In addition, the results were compared with the depth predictions made by skilled endoscopists.

**Results:** In the Radiomics study, the average cross-validation was 0.833. The mean AUC for cross-validation calculated from the receiver operating characteristic curve was 0.868. These results were equivalent to those of the diagnosis made by a skilled endoscopist.

**Conclusion:** The diagnosis of laryngopharyngeal cancer depth using radiomics analysis has potential clinical applications. We plan to use it in actual surgery in the future and prospectively study whether it can be used for diagnosis.

© 2023 Japanese Society of Otorhinolaryngology-Head and Neck Surgery, Inc. Published by Elsevier B.V. All rights reserved.

## 1. Introduction

Early-stage cancers are frequently detected not only in the gastrointestinal field but also in the laryngopharyngeal field with advances in optical technologies such as endoscopic diagnostic techniques, high-definition endoscopes, and magni-

\* Corresponding author.

E-mail address: [uedatsu@hiroshima-u.ac.jp](mailto:uedatsu@hiroshima-u.ac.jp) (T. Ueda).

fying endoscopy with narrow-band imaging (ME-NBI) [1–3]. Transoral surgery (TOS) is a minimally invasive procedure widely used to treat laryngopharyngeal cancer [4–7]. The range of indications for transoral surgery has expanded beyond superficial cancers to avoid adverse events caused by chemoradiotherapy, such as dysphagia and hypothyroidism, and to avoid loss of the larynx, other organs, and voice function caused by external incision surgery. Recently, transoral surgery has been performed for recurrent lesions after radiotherapy and for new lesions in the irradiated field. However, in some cases, it is difficult to determine the extent of horizontal and vertical resection during transoral surgery [8]. Currently, in clinical practice, depth prediction based on the morphology of the intrapapillary capillary loop (IPCL) using ME-NBI is applied to superficial laryngopharyngeal and esophageal carcinomas [9]. However, as the diagnosis is made by an endoscopist, it is expected that there will be no small differences in diagnostic ability among facilities due to clinical experience, sophistication of the institution, and other factors.

Medical image analysis using radiomics, an image analysis method based on artificial intelligence (AI), has progressed in recent years. Radiomics can systematically handle large amounts of image information in radiology by machine learning of a large number of quantified features, and has been applied to the screening, diagnosis, treatment, and evaluation of various types of tumors [10]. In the head and neck region, radiomic analysis and machine learning have been used to create predictive models of treatment efficacy [11].

In this study, we developed a predictive model for the depth diagnosis of pharyngeal laryngeal cancer based on pre-treatment images using radiomics' analysis. This is the first study to use radiomic analysis for the in-depth diagnosis of laryngopharyngeal carcinoma.

## 2. Materials and methods

### 2.1. Patients and endoscopic images

We included esophagogastroduodenoscopic images of 95 lesions that were pathologically diagnosed as squamous cell carcinoma (SCC) and treated with transoral surgery at our institution between August 2009 and April 2020. Of these, 54 lesions were SCC *in situ* and 41 were SCC. NBI images captured using a magnifying endoscope, H260Z or H290Z (Olympus Medical Systems Co., Ltd.), were used in this study. All examinations were performed by endoscopists with > 10 years of practical experience.

ME-NBI microvascular patterns were classified according to the Japan Esophageal Society (JES) Classification 6, which categorizes vessels as either type A or B. Type A vessels showed mild or no atypia of the IPCL (vessels with a diameter of 7–10  $\mu\text{m}$ ), while type B vessels showed obvious IPCL changes. Types A and B vessels strongly indicated intraepithelial neoplasia and SCC, respectively. Type B vessels were sub-classified into three groups as follows: type B1, dilated and tortuous vessels of various diameters and shapes with intact loop formation (dot-, spiral-, or waist-thread-like loop vessels of 20–30  $\mu\text{m}$ ); type B2, multi-layered and irreg-

ularly and dendritically branched vessels with no loop formation; and type B3, vessels that were visibly thicker than the surrounding vessels ( $\geq 3$ -fold thicker than B2 vessels, i.e., >60  $\mu\text{m}$  in diameter).

The JES Classification 6 is widely accepted in daily practice for the treatment of esophageal SCC in Japan. This classification can be used to determine the invasion depth of superficial laryngopharyngeal cancer (SPC). Accordingly, type B1 was defined as SPC limited to epithelial layer, while type B2/3 was defined as subepithelial layer.

All enrolled patients were informed of the risks and benefits of TOS and written informed consent was obtained for the use of their data. This study was approved by the Institutional Review Board of Hiroshima University Hospital (approval number: E-2039) and was conducted in accordance with the principles of the Declaration of Helsinki. The study protocol was posted at our institution, and all patients were given the choice to opt out of the study.

### 2.2. Method of TOS (endoscopic laryngopharyngeal surgery: ELPS) procedure (Fig. 1)

At our institution, transoral surgery is indicated for Tis, T1, T2, and T3 oropharyngeal, hypopharyngeal, and supraglottic cancers without cervical lymph node metastasis. In addition, we resected recurrent lesions after chemoradiotherapy if the lesions were relatively small and did not form ulcers. The resection margin was set differently for patients with low or high possibility of subepithelial invasion. If the possibility of subepithelial invasion was judged to be low (Type B1), horizontal margins were marked 2 and 3 mm outside the iodine unstained area and resected outside that zone, and vertical margins were resected to leave as much subepithelial tissue as possible. If the possibility of subepithelial invasion is judged to be high (Type B2,3), the horizontal section is marked 3 and 4 mm lateral to the iodine unstained area and resected outside it, and the vertical section is resected just above the muscle layer [12].

ELPS combines head and neck surgery and gastrointestinal endoscopic treatment. All examinations were performed by endoscopists with > 10 years of practical experience. All ELPSs procedures were performed by a head and neck surgeon and a gastroenterologist under general anesthesia with transoral or transnasal intubation. After placing the mouth-piece angle-wider, a curved rigid laryngoscope was inserted to lift the larynx and provide surgical view with the assistance of endoscopic vision. The surgical margin was carefully determined after obtaining an extended view of the magnifying endoscope with NBI (GIF-H260Z endoscope; Olympus, Tokyo, Japan) and iodine staining. Marking was performed approximately 2 and 3 mm from the edge of the lesion using an orally inserted electro-surgical needle knife (Disposable High Frequency Knife KD-600, Olympus, Tokyo, Japan). A head and neck surgeon orally injected a mixture of saline, indigo carmine, and epinephrine into the subepithelial layer. Lesions lifted by the curved grasping forceps inserted orally with adequate traction were dissected by a head and neck surgeon using an orally inserted curved electro-surgical needle

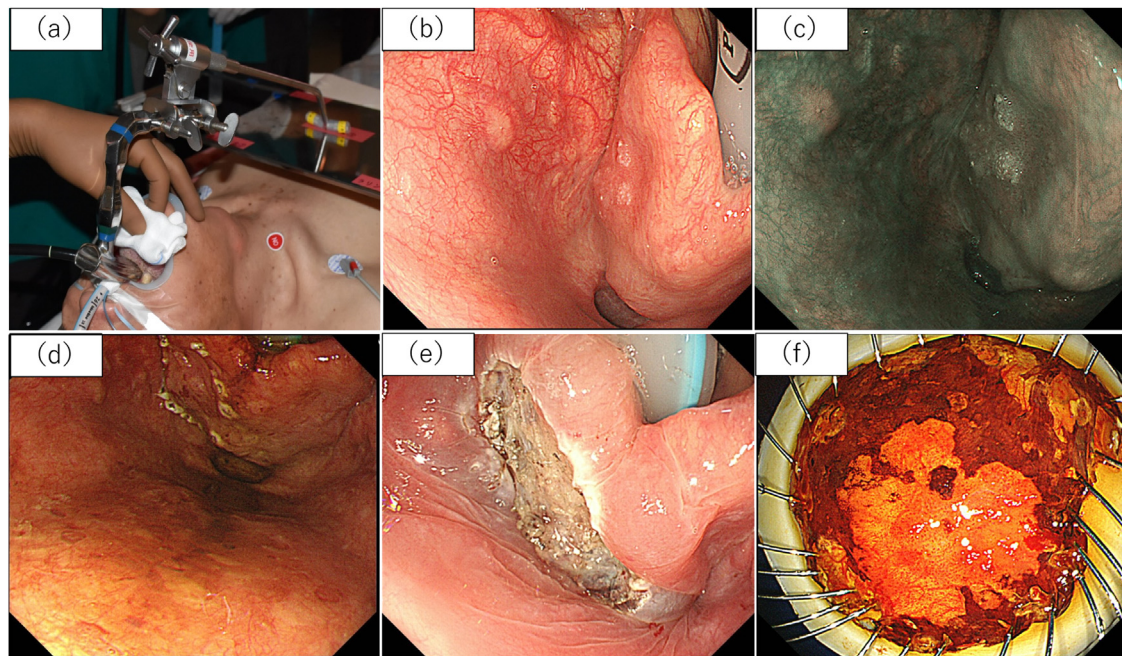


**Fig. 1.** Surgical procedure (Hypopharyngeal cancer Lt.PS TisN0M0).

(a) Laryngeal deployment (b) Observation with white lite (c) Observation with NBI  
(d) After marking (e) After resection (f) Excised specimen

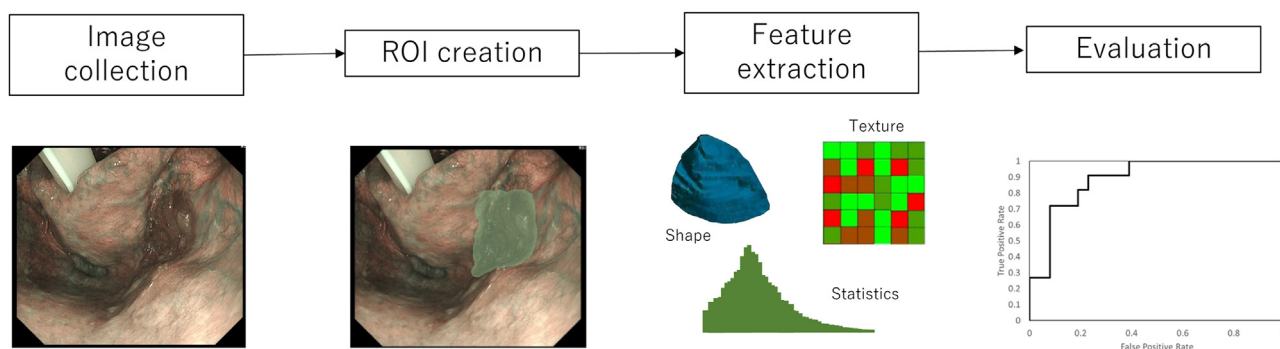


**Fig. 2.** The flow of the analysis using radiomics.

Medical images are collected, segmentation is performed on the medical images, and tumor regions are defined. From this region, features based on tumor intensity, texture, and shape are extracted. Finally, these features are used for analysis and machine learning is performed.

knife. In cases of operative difficulty due to endoscopy, forceps, or needle knife interruption, gastroenterologists directly resected the lesion using an endoscopic submucosal dissection (ESD) knife, with a head and neck surgeon assisting with adequate traction using forceps.

### 2.3. Analysis method

The workflow of this study is illustrated in Fig. 2. The NBI images obtained using esophagogastroduodenoscopy were transferred to a medical image computing tool (3D Slicer, [www.slicer.org](http://www.slicer.org), accessed on January 1, 2020). The lesion areas in the NBI images were manually delineated to create regions of interest (ROI). Segmentation was performed by two head and neck surgeons, including an expert. Radiomic features were extracted using an open-source package in Python and Pyradiomics software. A detailed list of radiomic features is provided in Table 1. The extracted radiomic features

included 13 shapes, 21 first-order, 50 quantitative, and 93 texture features. Textural features were extracted using low- and high-pass wavelet filters. A total of 837 radiomic features were extracted.

The most significant predictive features were selected using least absolute shrinkage and selection operator regression, which reduces the dimensions from among all candidate features in the training dataset.

We classified SCC and SCC *in situ* lesions with machine learning classifiers. The SCC and SCC *in situ* were labeled as 1 and 0, respectively. The machine learning classifiers used a neural network with rectified linear unit activation and ten hidden layers. Of the 95 patients, 71 and 24 were randomly assigned to the training and test datasets, respectively. A five-fold cross-validation method was used for training, and the diagnostic performance for the presence of subepithelial invasion was determined by verifying the correct response rate to distinguish SCC or SCC *in situ* as the predictive target



**Table 1.** Feature type and associated features.

| Feature type | Morphology -based          | First order-based              | Texture-based       |                                      |                                      |            |   |
|--------------|----------------------------|--------------------------------|---------------------|--------------------------------------|--------------------------------------|------------|---|
| Methods      | Shape                      | Histogram                      | GLCM                | GLSZM                                | GLRLM                                | NGTDM      | GLDM                                      |
| Feature name | Maximum 3D diameter        | Interquartile range            | Joint average       | Gray level variance                  | Short run low gray level emphasis    | Coarseness | Gray level variance                       |
|              | Maximum 2D diameter slice  | Skewness                       | Sum average         | Zone variance                        | Gray level variance                  | Complexity | High gray level emphasis                  |
|              | Sphericity                 | Uniformity                     | Joint entropy       | Gray level non uniformity normalized | Low gray level run emphasis          | Strength   | Dependence entropy                        |
|              | Minor axis                 | Median                         | Cluster shade       | Size zone non uniformity normalized  | Gray level non uniformity normalized | Contrast   | Dependence non uniformity                 |
|              | Elongation                 | Energy                         | Maximum probability | Size zone non uniformity             | Run variance                         | Busyness   | Gray level non uniformity                 |
|              | Surface volume ratio       | Robust mean absolute deviation | Idmn                | Gray level non uniformity            | Gray level non uniformity            |            | Small dependence emphasis                 |
|              | Volume                     | Mean absolute deviation        | Joint energy        | Large area emphasis                  | Long run emphasis                    |            | Small dependence high gray level emphasis |
|              | Major axis                 | Total energy                   | Contrast            | Small Area high gray level emphasis  | Short Run high gray level emphasis   |            | Dependence non uniformity normalized      |
|              | Surface area               | Maximum                        | Difference entropy  | Zone percentage                      | Run length non uniformity            |            | Large dependence emphasis                 |
|              | Flatness                   | Root mean squared              | Inverse variance    | Large area low gray level emphasis   | Short run emphasis                   |            | Large dependence low gray level emphasis  |
|              | Least axis                 | 90 percentile                  | Difference variance | Large area high gray level emphasis  | Long run high gray level emphasis    |            | Dependence variance                       |
|              | Maximum 2D diameter column | Minimum                        | Idn                 | High gray level zone emphasis        | Run percentage                       |            | Large dependence high gray level emphasis |
|              | Maximum 2D diameter row    | Entropy                        | Idm                 | Small area emphasis                  | Long run low gray level emphasis     |            | Small dependence low gray level emphasis  |
|              |                            | Range                          | Correlation         | Low gray level zone emphasis         | Run entropy                          |            | Low gray level emphasis                   |
|              |                            | Variance                       | Autocorrelation     | Zone entropy                         | High gray level run emphasis         |            |   |
|              |                            | 10 percentile                  | Sum entropy         | Small area low gray level emphasis   | Run length non uniformity normalized |            |   |
|              |                            | Kurtosis Mean                  | Sum squares         |                                      |                                      |            |   |
|              |                            |                                | Cluster prominence  |                                      |                                      |            |   |
|              |                            |                                | Imc2                |                                      |                                      |            |   |
|              |                            |                                | Imc1                |                                      |                                      |            |   |
|              |                            |                                | MCC                 |                                      |                                      |            |   |
|              |                            |                                | Difference average  |                                      |                                      |            |   |
|              |                            |                                | Id                  |                                      |                                      |            |   |
|              |                            |                                | Cluster tendency    |                                      |                                      |            |   |



Fig. 3. Training and testing process. Fivefold cross-validation was built.

Table 2. Patient and lesion characteristics.

|                        |                |           |
|------------------------|----------------|-----------|
| Sex                    |                |           |
| Male                   |                | 88(92.6%) |
| Female                 |                | 7(7.4%)   |
| Age (year,mean±SD)     |                |           |
|                        |                | 65.2±10.2 |
| Location               |                |           |
| Hypopharynx            |                | 72(75.8%) |
|                        | pyriform sinus | 58(61.1%) |
|                        | posterior wall | 8(8.4%)   |
|                        | postcricoid    | 6(6.3%)   |
| Oropharynx             |                | 18(18.9%) |
|                        | posterior wall | 10(10.5%) |
|                        | anterior wall  | 5(5.3%)   |
|                        | side wall      | 2(2.1%)   |
|                        | upper wall     | 1(1.0%)   |
| Larynx                 |                | 5(5.3%)   |
|                        | supraglottic   | 5(5.3%)   |
| ME-NBI                 |                |           |
| type B1                |                | 75(79.0%) |
| type B2                |                | 19(20.0%) |
| type B3                |                | 1(1.0%)   |
| Pathological diagnosis |                |           |
| SCC <i>in situ</i>     |                | 54(56.8%) |
| SCC                    |                | 41(43.2%) |

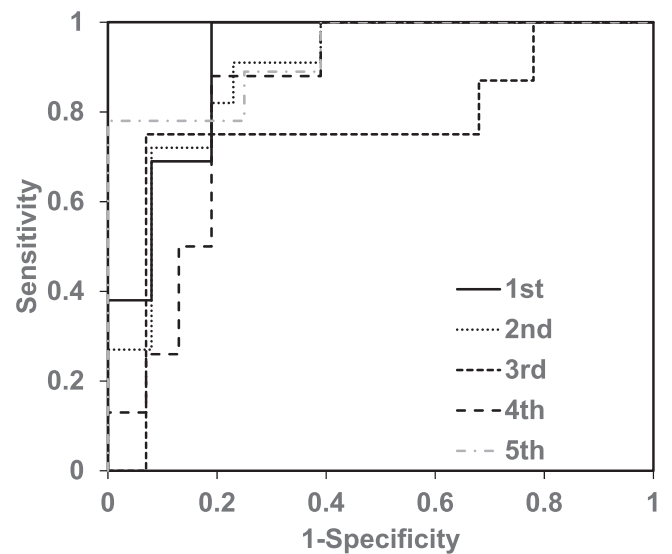


Fig. 4. The model performance was evaluated with the ROC

(Fig. 3). Predictive performance was evaluated using accuracy, sensitivity, specificity, and area under the receiver operating characteristic (ROC) curve (AUC).

### 3. Results

#### 3.1. Patient and lesion characteristics

The characteristics of the 95 lesions are shown in Table 2. There were 88 males and 7 females. The median age of the patients was 65 years. The performance status (PS) was 0 (85 lesions) or 1 (10 lesions), and no patient had a PS 2. The most

common location was the hypopharynx (72 lesions, 75.8%), followed by the oropharynx (18 lesions, 18.9%) and larynx (5 lesions, 5.3%). Intraoperatively, each lesion was diagnosed by an endoscopist with over 10 years of clinical experience, based on the Japanese Classification of Esophageal Cancer (11th edition). 75 lesions (79.0%) were Type B1, 19 (20.0%) were Type B2, and 1 (1.0%) was Type B3. All patients underwent transoral surgery for these lesions; 54 had SCC *in situ*, and 41 had SCC.

#### 3.2. Analysis

The accuracy, sensitivity, specificity and AUC of diagnosing SCC *in situ* by radiomics analysis were calculated. Fig. 4 shows the performance of the prediction model based on the ROC curve and Table 3 shows the Accuracy, Sensi-

**Table 3.** The accuracy, sensitivity, specificity, and AUC of diagnosing SCC *in situ* calculated from the ROC with Radiomics.

|         | Accuracy | Sensitivity | Specificity | AUC   |
|---------|----------|-------------|-------------|-------|
| 1st     | 87.5%    | 81.8%       | 92.3%       | 0.916 |
| 2nd     | 83.3%    | 92.3%       | 72.7%       | 0.889 |
| 3rd     | 79.2%    | 81.3%       | 75.0%       | 0.765 |
| 4th     | 75.0%    | 81.3%       | 62.5%       | 0.841 |
| 5th     | 91.7%    | 100.0%      | 77.8%       | 0.93  |
| Average | 83.3%    | 87.3%       | 76.1%       | 0.868 |

tivity, Specificity, and AUC calculated from the ROC curve. The average accuracy, sensitivity, specificity, and area under the curve were 83.3 %, 87.3%, 76.1%, and 0.868, respectively. Table 4 shows the features selected as predictors in the radiomic analysis.

Table 5 shows a comparison of tumor depth between ME-NBI and the pathological diagnosis. 75 lesions were classified as type B1 using ME-NBI, of which 54 (72%) were SCC *in situ* and 21 (28%) were SCC. The accuracy, sensitivity, and specificity for the *in situ* diagnosis of SCC were 77.9%, 100%, and 48.8%, respectively (Table 6).

#### 4. Discussion

To the best of our knowledge, this is the first study to investigate a predictive diagnostic model using radiomic analysis for preoperative depth diagnosis of laryngopharyngeal cancer.

In recent years, the application of AI in medicine has rapidly advanced, particularly in diagnostic imaging studies.

Radiomics has attracted significant attention as a method for medical image analysis using AI [10]. The workflow of radiomics was as follows. Medical images were collected as data, segmented, and the tumor regions were defined. From this region, features based on the tumor intensity, texture, and shape were extracted. Finally, these features were used for analysis and machine learning was performed. Radiomic analysis can reveal predictive imaging features. It has the potential to overcome interobserver variability in visual assessment and yield useful predictive features that cannot be discriminated by visual analysis [13]. The novelty of this study lies in the development of a system that can complement depth assessment of malignant lesions, which has until now depended on the endoscopist's diagnostic ability. In addition, radiomic analysis has been reported in laryngopharyngeal region for modalities such as CT and MRI [14,15], but not so far for endoscopic images. Radiomic analysis can reveal predictive imaging features, but it was not clear what the features selected as predictors in this study meant. Future work is needed to analyze the clinical or biological features implied by imaging features in an understandable manner.

Early detection of pharyngeal cancer during endoscopic diagnosis is important because the treatment of advanced pharyngeal cancer significantly reduces the quality of life [16–18]. Although TOS, including ELPS, is widely used for the treatment of superficial cancer of the pharynx [19–23], there are some cases in which it is difficult to set vertical margins

using only endoscopic findings, and some cases with positive vertical margins have unfortunate outcomes. Dysphagia after transoral surgery for superficial pharyngeal carcinoma is a serious complication that affects the patient's postoperative quality of life [22,23]. The extent of resection in TOS is an important consideration, as excessive resection leads to postoperative scarring and adhesions, and increases complications.

Currently, in clinical practice, depth prediction based on the morphology of the IPCL by ME-NBI has been applied to superficial cancers of the pharynx as well as superficial cancers of the esophagus [9,12], it is expected that there are some differences in diagnostic performance between institutions, depending on the clinical experience and sophistication of the endoscopist making the diagnosis. There are also reports indicating that there is room for improvement in the depth of diagnosis of superficial esophageal cancer [24]. Other devices and improved endoscopic diagnostic accuracy may be needed, and in this study, we investigated whether AI could be used to provide a highly accurate depth diagnosis of laryngopharyngeal carcinoma from preoperative images. In addition, we compared the ability of skilled endoscopists to diagnose the depth with that of AI. The endoscopist's diagnosis showed subepithelial invasive carcinoma in 28% of lesions diagnosed as type B1, whereas all lesions diagnosed as type B2 or higher were subepithelial invasive carcinoma, suggesting that while a diagnosis of subepithelial invasive carcinoma can be made if type B2 or higher findings are found within the lesion, it is possible that some lesions classified as type B1 in the preoperative diagnosis may also show subepithelial invasion, and careful observation by ME-NBI is essential during TOS. Referring to the AI depth diagnosis results, the accuracy was comparable to that of the endoscopist's diagnosis, with inferior sensitivity but superior specificity. This suggests that an AI-based depth diagnosis system can complement the diagnosis by endoscopists. It has also been reported that depth prediction using AI is highly accurate for gastric cancer [25]. Although there is a possibility that there will be some variation among institutions in terms of the manual creation of ROIs around lesions, the system is expected to be versatile except for this point. If the system can be improved to a system that can automatically recognize lesions, create ROIs, and reach a diagnosis, it may be possible to apply the system to endoscopes in actual clinical practice. The development of endoscopic instruments with such depth diagnostic systems could lead to a reduction in the number of cases of positive deep margins and cases of postoperative dysphagia. In addition, we reported the usefulness of transoral ultrasonography for depth assessment in laryngopharyngeal cancer, and further improvements in predictive performance can be expected when other modalities are also used [26].

This study has some limitations. The study population was recruited from a single center, and the number of patients included was relatively limited. Further studies involving more lesions are needed to improve the accuracy of depth diagnosis. In addition, the case series in this study were not classified by site and included cancers throughout the laryngopharyngeal region. Since depth diagnosis by AI is based on factors other than visual diagnosis by humans, all of them were ex-

**Table 4.** Features selected as predictors in Radiomics analysis.

|            |                                  | 0           | 1           |
|------------|----------------------------------|-------------|-------------|
| firstorder | Median                           | 5.491811899 | 2.826286919 |
| firstorder | Minimum                          | 0.083203306 | 0.071058273 |
| glrlm      | GrayLevelNonUniformityNormalized | 0.237168126 | 0.194784496 |
| glrlm      | RunEntropy                       | 1.868150738 | 2.464910981 |
| glcm       | ClusterShade                     | 23.90759689 | 27.96747376 |
| glszm      | GrayLevelNonUniformityNormalized | 41.47784575 | 19.21356981 |
| glszm      | GrayLevelVariance                | 571.9841517 | 320.2106263 |
| glszm      | SizeZoneNonUniformityNormalized  | 4.99884863  | 4.794072765 |
| glszm      | ZoneEntropy                      | 4270.619909 | 6205.852298 |
| ngtdm      | Complexity                       | 0.263875143 | 0.336519254 |

**Table 5.** Comparison of ME-NBI and pathological diagnosis.

|            | SCC <i>in situ</i> | SCC      | total |
|------------|--------------------|----------|-------|
| type B1    | 54(72%)            | 21(28%)  | 75    |
| type B2,B3 | 0(0%)              | 20(100%) | 20    |

**Table 6.** The accuracy, sensitivity, specificity, and AUC of diagnosing SCC *in situ* by ME-NBI.

|             |       |
|-------------|-------|
| Sensitivity | 100%  |
| Specificity | 48.8% |
| Accuracy    | 77.9% |

amined in this study. Nor were they classified according to whether or not there was prior treatment for head and neck lesions. Similarly, depth diagnosis by AI is based on factors other than where humans visually diagnose, so we considered all of them in this study.

With this AI analysis, we plan to examine whether there is a difference in diagnosis by site or treatment history in the future.

## 5. Conclusion

This study suggests that AI-based predictive models may be useful for diagnosing the depth of laryngopharyngeal cancer. This is the first article to use radiomics analysis for depth diagnosis of pharyngeal laryngeal cancer. These results may complement depth diagnosis by skilled endoscopists and have great potential for clinical applications.

## Funding

This study was supported by JSPS KAKENHI (Grant Number 20K09713).

## Ethical issues

The Institutional Review Board of Hiroshima University Hospital approved this study (Hiroshima University Hospital IRB E-2039).

## Author contributions

Contributor TU was responsible for the organization and coordination of the trial. TU was the chief investigator and

DK and KY were responsible for the data analysis. TU and DK developed the trial design. DK and KY were writing original draft. TU was writing review and editing. All authors contributed to the writing of the final manuscript.

## Declaration of Competing Interest

The authors declare that they have no conflicts of interest.

## References

- [1] Muto M, Katada C, Sano Y, Yoshida S. Narrowband imaging: a new diagnostic approach to visualize angiogenesis in the superficial neoplasm. *Clin Gastroenterol Hepatol* 2005;3(Supplement 1):S16–20. doi:10.1016/s1542-3565(05)00262-4.
- [2] Muto M, Nakane M, Katada C, Sano Y, Ohtsu A, Esumi H, et al. Squamous cell carcinoma *in situ* at oropharyngeal and hypopharyngeal mucosal sites. *Cancer* 2004;101:1375–81. doi:10.1002/cncr.20482.
- [3] Muto M, Minashi K, Yano T, Saito Y, Oda I, Nonaka S, et al. Early detection of superficial squamous cell carcinoma in the head and neck region and esophagus by narrow band imaging: a multi-center randomized controlled trial. *J Clin Oncol* 2010;28:1566–72. doi:10.1200/JCO.2009.25.4680.
- [4] Sato H, Tsukahara K, Okamoto I, Katsube Y, Yagi K, Yamaguchi H, et al. Short-term clinical results of transoral endoscopic laryngopharyngeal surgery for superficial laryngopharyngeal carcinoma. *Nihon Jibiinkoka Gakkai Kaiho* 2019;122:891–7. doi:10.3950/jibiinkoka.122.891.
- [5] Tateya I, Muto M, Morita S, Miyamoto S, Hayashi T, Funakoshi M, et al. Endoscopic laryngo-pharyngeal surgery for superficial laryngo-pharyngeal cancer. *Surg Endosc* 2016;30:323–9. doi:10.1007/s00464-015-4213-y.
- [6] Watanabe A, Taniguchi M, Kimura Y, Hosokawa M, Ito S, Tsukamoto S, et al. Synopsis of transoral endoscopic laryngopharyngeal surgery for superficial pharyngeal cancers. *Head Neck* 2017;39:1779–87. doi:10.1002/hed.24839.
- [7] Nakayama M, Katada C, Mikami T, Okamoto M, Koizumi W, Tanabe S, et al. A clinical study of transoral pharyngectomies to treat superficial hypopharyngeal cancers. *Jpn J Clin Oncol* 2013;43:782–7. doi:10.1093/jjco/hyt081.
- [8] Eguchi K, Matsui T, Mukai M, Sugimoto T. Prediction of the depth of invasion in superficial pharyngeal cancer: microvessel morphological evaluation with narrowband imaging. *Head Neck* 2019;41:3970–5. doi:10.1002/hed.25935.
- [9] Japan Esophageal Society. Japanese classification of esophageal cancer. 11th ed. 2017;14.
- [10] Lambin P, Rios-Velazquez E, Leijenaar R, Carvalho S, van Stiphout RG, Granton P, et al. Radiomics: extraction of additional information from medical images using advanced feature analysis. *Eur J Cancer* 2012;48:441–6. doi:10.1016/j.ejca.2011.11.036.

- [11] Peng Z, Wang Y, Wang Y, Jiang S, Fan R, Zhang H, et al. Application of radiomics and machine learning in head and neck cancers. *Int J Biol Sci* 2021;17:475–86. doi:[10.7150/ijbs.55716](https://doi.org/10.7150/ijbs.55716).
- [12] Ueda T, Yumii K, Urabe Y, Chikuie N, Takumida M, Taruya T, et al. Examination of micro-superficial lesions of up to 5 mm in size in the pharyngolaryngeal region. *J Laryngol Otol* 2022;1–8. doi:[10.1017/S0022215122001761](https://doi.org/10.1017/S0022215122001761).
- [13] Mayerhoefer ME, Materka A, Langa G, Häggström I, Szczypiński P, Gibbs, et al. Introduction to radiomics. *J Nucl Med* 2020;61:488–95. doi:[10.2967/jnumed.118.222893](https://doi.org/10.2967/jnumed.118.222893).
- [14] Kubo K, Kawahara D, Murakami Y, Takeuchi Y, Katsuta T, Imano N, et al. Development of a radiomics and machine learning model for predicting occult cervical lymph node metastasis in patients with tongue cancer. *Oral Surg Oral Med Oral Pathol Oral Radiol* 2022;134:93–101. doi:[10.1016/j.oooo.2021.12.122](https://doi.org/10.1016/j.oooo.2021.12.122).
- [15] Akram F, Koh PE, Wang F, Zhou S, Tan SH, Paknezhad M, et al. Exploring MRI based radiomics analysis of intratumoral spatial heterogeneity in locally advanced nasopharyngeal carcinoma treated with intensity modulated radiotherapy. *PLoS One* 2020;15:e0240043. doi:[10.1371/journal.pone.0240043](https://doi.org/10.1371/journal.pone.0240043).
- [16] Kinjo Y, Nonaka S, Oda I, Abe S, Suzuki H, Yoshinaga S, et al. The short-term and long-term outcomes of the endoscopic resection for the superficial pharyngeal squamous cell carcinoma. *Endosc Int Open* 2015;3:E266–73. doi:[10.1055/s-0034-1392094](https://doi.org/10.1055/s-0034-1392094).
- [17] Eckel HE, Staar S, Volling P, Sittel C, Damm M, Jungehuelsing M, et al. Surgical treatment for hypopharynx carcinoma: feasibility, mortality, and results. *Otolaryngol Head Neck Surg* 2001;124:561–9. doi:[10.1067/mhn.2001.115060](https://doi.org/10.1067/mhn.2001.115060).
- [18] Johansen LV, Grau C, Overgaard J. Hypopharyngeal squamous cell carcinoma-treatment results in 138 consecutively admitted patients. *Acta Oncol* 2000;39:529–36. doi:[10.1080/028418600750013465](https://doi.org/10.1080/028418600750013465).
- [19] Tateya I, Muto M, Morita S, Miyamoto SI, Hayashi T, Funakoshi M, et al. Endoscopic laryngo-pharyngeal surgery for superficial laryngopharyngeal cancer. *Surg Endosc* 2016;30:323–9. doi:[10.1007/s00464-015-4213-y](https://doi.org/10.1007/s00464-015-4213-y).
- [20] Watanabe A, Taniguchi M, Kimura Y, Hosokawa M, Ito S, Tsukamoto S, et al. Synopsis of transoral endoscopic laryngopharyngeal surgery for superficial pharyngeal cancers. *Head & Neck* 2017;39:1779–87. doi:[10.1002/hed.24839](https://doi.org/10.1002/hed.24839).
- [21] Nakayama M, Katada C, Mikami T, Okamoto M, Koizumi W, Tanabe S, et al. A clinical study of transoral pharyngectomies to treat superficial hypopharyngeal cancers. *Jpn J Clin Oncol* 2013;43(8):782–7. doi:[10.1093/jjco/hyt081](https://doi.org/10.1093/jjco/hyt081).
- [22] Fujiwara K, Taira K, Donishi R, Koyama S, Morisaki T, Fukuhara T, et al. Preoperative predictors of dysphagia after transoral surgery. *Int J Clin Oncol* 2021;26:835–40. doi:[10.1007/s10147-021-01860-9](https://doi.org/10.1007/s10147-021-01860-9).
- [23] Ueda T, Yumii K, Urabe Y, Chikuie N, Taruya T, Kono T, et al. Swallowing function after transoral surgery for laryngopharyngeal cancer. *PLoS One* 2022;17:e0270509. doi:[10.1371/journal.pone.0270509](https://doi.org/10.1371/journal.pone.0270509).
- [24] Chino O, Makuuchi H, Shimada H. Diagnosis of the invasion depth of superficial esophageal carcinoma. *Gastroenterol Endosc* 2015;57:1243–53.
- [25] Cao R, Tang L, Fang M, Zhong L, Wang S, Gong L, et al. Artificial intelligence in gastric cancer: applications and challenges. *Gastroenterol Rep* 2022;1–16. doi:[10.1093/gastro/goac064](https://doi.org/10.1093/gastro/goac064).
- [26] Yumii K, Ueda T, Urabe Y, et al. Determining invasion depth in superficial pharyngeal carcinoma by transoral ultrasonography. *Laryngoscope* 2023;133:2192–7. doi:[10.1002/lary.30483](https://doi.org/10.1002/lary.30483).